Multi-Band Wireless Access-and-Backhaul (WAB) for 5G: Implementation and Experiments

Chiara Rubaltelli, Marcello Morini, Eugenio Moro, Ilario Filippini
Dipartimento di Elettronica, Informazione e Bioingegneria, Politecnico di Milano, Milan, Italy
name.surname@polimi.it

Abstract—The growing demand for wireless capacity and coverage has driven research into new radio architectures and higher frequency bands. The recently standardized Wireless Access Backhaul (WAB) architecture represents a key evolution, enabling cost-effective network densification through wireless relaying. This paper presents the first experimental realization of a multi-band WAB testbed, combining an FR2 backhaul and an FR1 access link using open-source software and commercial offthe-shelf components. The proposed framework validates the feasibility of end-to-end WAB operation and demonstrates its ability to extend FR2 coverage while maintaining compatibility with legacy FR1 user equipment. Experimental campaigns conducted in vehicular and outdoor-to-indoor scenarios confirm that WAB effectively mitigates the limitations of FR2 links, particularly in uplink and Non-Line-of-Sight conditions. These results highlight WAB as a practical and scalable approach for next-generation wireless networks.

Index Terms—Wireless Access and Backhaul (WAB), FR1/FR2 system, 3GPP RAN architectures, SDR testbed.

I. Introduction

The growing demand for bandwidth and spectral efficiency in wireless networks has intensified research into new frequency bands and novel Radio Access Network (RAN) architectures for 5G. Network densification is a key enabler to sustain this continuous growth in radio access capacity demand. In addition, it facilitates the adoption of higher frequency bands for radio access, such as Frequency Range 2 (FR2, 24.25–71 GHz) introduced by 3rd Generation Partnership Project (3GPP), which offers wide bandwidths and supports multi-Gbps data rates. However, FR2 communications suffer from severe path loss, high penetration losses, and strong susceptibility to environmental factors [1].

To achieve cost-effective network densification through wireless relaying, 3GPP introduced the concept of Integrated Access and Backhaul (IAB) in Release 15 [2]. IAB enables multi-hop topologies in which a donor node provides wireless backhaul connectivity to IAB nodes, which can in turn act as parent nodes to other IAB nodes or directly serve User Equipments (UEs). Each IAB node comprises a Mobile Termination (MT), used for connecting to the donor or parent node over the backhaul link, and a Distributed Unit (DU), responsible for providing access to UEs or child nodes.

However, IAB systems face significant implementation complexity and limited flexibility, which have hindered their large-scale adoption. Mobility procedures are rigid and verbose [3], centralized and full network control is required, and resource management must be tightly integrated with that of

the donor. These challenges become increasingly severe as the number of hops grows. In addition, despite several analytical and simulation-based studies, practical IAB experimental frameworks remain scarce ([4], [5]), and to the best of our knowledge, only experimental or pre-commercial IAB nodes have been mentioned in limited reports. The added complexity of IAB, combined with the lack of real-world validation, appears to be the main obstacle to its market deployment.

To address these limitations, 3GPP Release 19 introduces the Wireless Access Backhaul (WAB) architecture [6]. WAB retains the use of wireless backhaul while simplifying both the overall architecture and associated procedures. Each WAB node integrates a MT with a complete Next Generation NodeB (gNB), thereby providing direct access to UEs. Its modular design supports multiple backhaul technologies, including Non-Terrestrial Networks (NTNs), and introduces full independence between the access and backhaul segments. These features enable multi-band operation, allowing flexible combinations of the high throughput of FR2 communications with the superior penetration and wider device compatibility of FR1, thus mitigating high-frequency coverage limitations and ensuring support for legacy devices.

Although WAB represents a promising evolution, no physical implementation has been publicly documented to date. This paper addresses this gap by presenting the first multi-band WAB testbed, which integrates a commercial FR2 backhaul with an FR1 access segment using open-source software, Software-defined Radios (SDRs), and commercial components. The proposed testbed, assembled from standard components requiring only minor modifications, demonstrates that implementing the WAB architecture can be achieved rapidly and cost-effectively using existing technological expertise. These results suggest that the widespread adoption of WAB may be closer to realization than previously anticipated.

Leveraging this testbed, we conducted an experimental campaign to validate the proposed system in urban vehicular and Outdoor to Indoor (O2I) scenarios, confirming its potential to extend FR2 benefits while mitigating typical propagation impairments. This initial campaign already highlights the main advantages of wireless backhaul. In particular, our results demonstrate that the WAB architecture can effectively overcome the limitations of uplink transmissions, providing enhanced performance even in challenging Non-Line of Sight (NLoS) indoor environments.

The remainder of this paper is organized as follows. Sec-

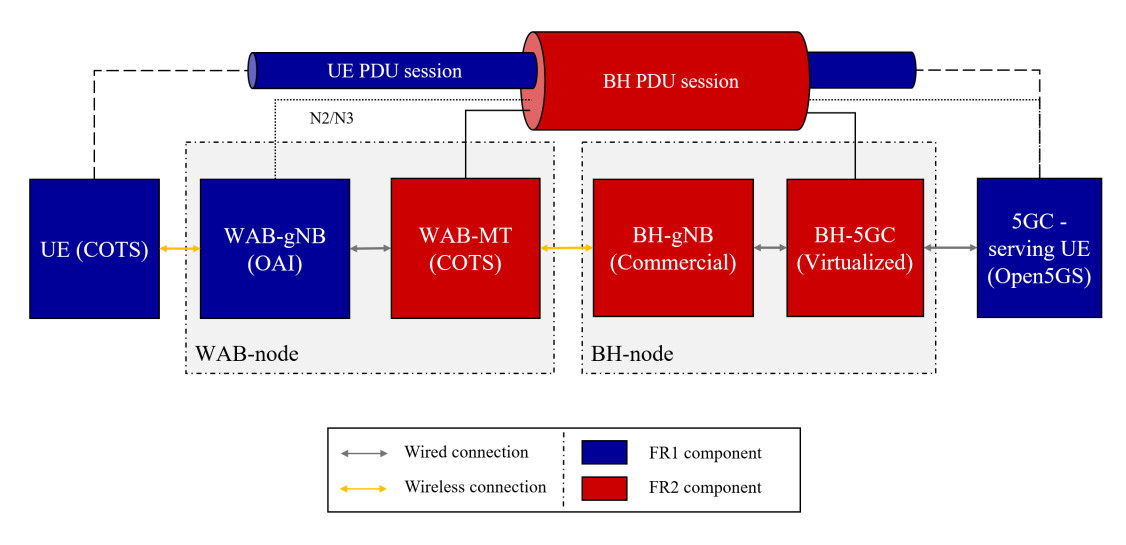


Fig. 1: WAB's fundamental architecture, including the corresponding elements in the testbed.

tion II outlines the WAB architecture and its fundamental operations. Section III details the proposed multi-band testbed and its main components. Section IV presents the experimental campaign and discusses the obtained results. Finally, Section V concludes the paper and highlights future research directions.

II. WIRELESS ACCESS BACKHAUL

The year 2025 marked the standardization of WAB as a topological enhancement for 5G-Advanced (5G-A) [7]. Similarly, Mobile Wireless Access Backhaul (MWAB) has been standardized as an architectural enhancement for Vehicle-Mounted Relays (VMR) [8]. Although defined by different Working Groups (WGs), the two technologies share the same architectural foundation, which we describe in the following, together with some basic procedures.

A. Architecture

The WAB architecture comprises two communication systems: one for radio access and one for wireless backhaul. These can operate in either in-band or out-of-band configurations, with the objective of providing end-to-end connectivity through wireless backhaul. A schematic representation of the basic architecture is shown in Fig. 1.

One of the core elements of the WAB architecture is the WAB Node, which consists of a WAB-gNB and a WAB Mobile Termination (WAB-MT). The WAB-gNB is a standard-compliant 5G Base Station (BS) that provides radio access to UEs, while the WAB-MT – supporting a subset of UE functionalities – establishes a wireless connection with the BH-gNB. This connection is used by the WAB-gNB as a backhaul link to the Core Network (CN) (5GC-Serving-UE).

Each WAB Node is associated with a donor node, referred to as the BH node, which includes the BH-gNB and a BH-5GC. In the basic configuration, the BH-gNB is also a 5G standard-compliant BS, providing connectivity to the WAB-MT through conventional radio access procedures and resources. The BH-gNB is locally connected to the BH-5GC, whose N6 interface

links to the 5GC-Serving-UE. Alternatively, the backhaul segment can be implemented using a non-3GPP link or network.

In both cases, the end UEs remain agnostic to the underlying backhaul mechanisms, maintaining full service transparency. This feature enables the extension of 5G coverage through heterogeneous or non-3GPP infrastructures.

The WAB architecture enables end-to-end connectivity for the end UE by tunneling the N2 and N3 interfaces – linking the WAB-gNB to the 5GC-Serving-UE – through BH Packet Data Unit (PDU) sessions established between the WAB-MT and the BH-5GC. In the control plane, the wireless backhaul is provided through a BH PDU session that carries the N2 interface connecting the WAB-gNB to the 5GC-Serving-UE's Access and Mobility Management Function (AMF). Similarly, in the user plane, data are transmitted over a separate BH PDU session supporting the N3 interface between the WAB-gNB and the 5GC-Serving-UE's User Plane Function (UPF).

The backhaul (red in Fig. 1) and access (blue in Fig. 1) segments operate as two logically independent 5G networks. The BH network provides backhaul connectivity to the WAB-MT, while the access network serves the end UE. The BH network can be implemented over either a Terrestrial Network (TN) or a NTN; in both cases, 5G access remains guaranteed regardless of the backhaul's underlying technology.

B. Basic Procedures

The WAB-node attachment – or WAB-node integration – procedure begins with the setup of the WAB-MT, which connects to the BH-gNB as a standard UE using conventional 5G access procedures. Once authorized by the BH-5GC, the WAB-MT establishes one or more BH PDU sessions with the BH-5GC's UPF. Multiple BH PDU sessions can be created to transport different logical interfaces or to enable differentiated traffic handling based on Quality of Service (QoS) requirements. These sessions constitute the foundation for carrying traffic from the WAB-gNB and its connected UEs.

Following the WAB-MT setup, the WAB-gNB is initialized and registers with the 5GC-Serving-UE, thereby enabling the

establishment of PDU sessions for connected UEs. Specifically, each UE PDU session is supported by a Data Radio Bearer (DRB) between the UE and the WAB-gNB, and by a conventional N3 GPRS Tunneling Protocol (GTP) tunnel between the WAB-gNB and the 5GC-Serving-UE. The latter is encapsulated within the BH PDU session tunnels established during the WAB-node integration phase.

Through the Xn interface, the WAB-gNB can establish connections with neighboring gNBs. These connections are tunneled through the BH network and may terminate either at the BH-gNB providing access to its co-located WAB-MT or at other gNBs connected to the 5GC-Serving-UE.

As the WAB node moves, the WAB-MT follows legacy UE mobility procedures, enabling seamless handovers within the BH network. Moreover, the WAB-MT can request or modify BH PDU sessions on demand from the WAB-gNB as it moves across the network. To prevent multi-hop across mobile WAB nodes, a WAB-MT is not allowed to hand over to a target WAB-gNB. This leads to star-like, single-hop logical topologies interconnecting mobile WAB nodes with the donor node. Single-hop connectivity, however, does not necessarily affect the BH network, which can employ any underlying technology or topology to support the user- and control-plane tunneling required by mobile WAB nodes.

Free mobility and seamless BH handovers are the two key features that distinguish the WAB architecture from similar solutions, such as NR femtocells, which are primarily designed to provide NR access in residential or enterprise environments.

III. WAB EXPERIMENTAL FRAMEWORK

The realized testbed aligns with the fundamental architecture of WAB systems and the corresponding components are displayed in Fig. 1 (in brackets). The experimental setup implements a multi-band WAB configuration, where the access system – connecting UE and WAB-gNB – operates at FR1, while the backhaul system – connecting WAB-MT and BH-gNB – works at FR2.

A detailed description of the testbed components is provided below, highlighting how they implement a 3GPP-compliant, fully functional WAB system using open-source software and commercial hardware, ensuring compatibility with Commercial Off-the-Shelf (COTS) UEs. The assembly required no hardware modifications beyond standard 5G components. This simplicity is key to achieving rapid and cost-effective deployment, thereby facilitating the widespread adoption of WAB technology.

a) FR2 components: The FR2 system components are part of the High-Frequency Campus Lab (HFCL) [9], an open and standard-compliant FR2 5G network deployed at Politecnico di Milano. Specifically, the WAB-MT is implemented using a COTS Customer Premises Equipment (CPE). The BH-gNB's Active Antenna Unit (AAU) is installed at a height of 22 m on a building rooftop and is interfaced via a 25 Gbps eCPRI fiber fronthaul to a Base Band Unit (BBU). The BBU is connected to a virtualized commercial 5G Core (5GC) (BH-5GC) through a 10 Gbps backhaul link.

The system operates at a center frequency of 27.2 GHz, with a channel bandwidth of 200 MHz and a subcarrier spacing of 120 kHz. The frame structure follows a Time Division Duplexing (TDD) 4:1 configuration. The AAU provides an Effective Isotropic Radiated Power (EIRP) of 70 dBm with an 8T8R Multiple Input, Multiple Output (MIMO) configuration, while the CPE operates with an EIRP of 40 dBm and a 2T2R MIMO configuration. Further details on the FR2 system are available in [9]. The FR2 network is used exclusively for research purposes and was entirely dedicated to the testbed, without any additional traffic.

b) FR1 components: The UE used in the testbed is a COTS 5G smartphone operating in FR1. The WAB-gNB is implemented using an OpenAirInterface (OAI) gNB, deployed on a laptop equipped with a SDR. OAI is an open-source platform that enables the deployment of a 5G RAN on general-purpose hardware, which can be connected to SDRs to provide wireless access to commercial UEs [10].

The FR1 gNB operates with 40 MHz bandwidth and a subcarrier spacing of 30 kHz in a SISO configuration. The maximum transmission power is 20 dBm, and the TDD configuration follows a 4:1 downlink-to-uplink split. The WAB-gNB laptop is connected to the WAB-MT via an Ethernet link. Finally, the 5GC-Serving-UE consists of an Open5GS Core instance installed on a general-purpose server connected to the BH-5GC. Open5GS is an open-source implementation of the 5GC, composed of virtualized Network Functions.

c) Connectivity: Once all components were assembled into the final WAB testbed, connectivity was established as follows. Since the 5GC-Serving-UE could not be directly reached by the WAB-gNB due to the CPE Network Address Translation (NAT) mechanism, a Virtual Private Network (VPN) tunnel was deployed to transport the N2 and N3 interfaces between the 5GC-Serving-UE and the WAB-gNB. This configuration reflects real-world deployments, where the N2 and N3 interfaces are typically protected from direct exposure to external networks. Some adjustments to the tunnel configuration were required to optimize performance. In particular, the Maximum Transmission Unit (MTU) size was reduced from 1420 bytes to 1384 bytes, as suggested in [11].

In summary, the proposed setup employs three levels of encapsulation to ensure proper end-to-end connectivity: the BH PDU tunnel encapsulates the VPN tunnel transporting the N2 and N3 interfaces, which in turn carries the PDU sessions of the end UEs.

IV. VALIDATION AND RESULTS

Dense urban environments challenge high-frequency signals in the FR2 band, where buildings and obstacles cause severe penetration and propagation losses. Multi-band WAB technology mitigates these effects by combining FR2 and FR1 links to extend coverage and improve reliability. In particular, an FR1 hop can overcome blockages that would otherwise disrupt FR2-only connectivity.

To support these considerations, we conducted an extensive experimental campaign in mobile and O2I scenarios. Figure 2

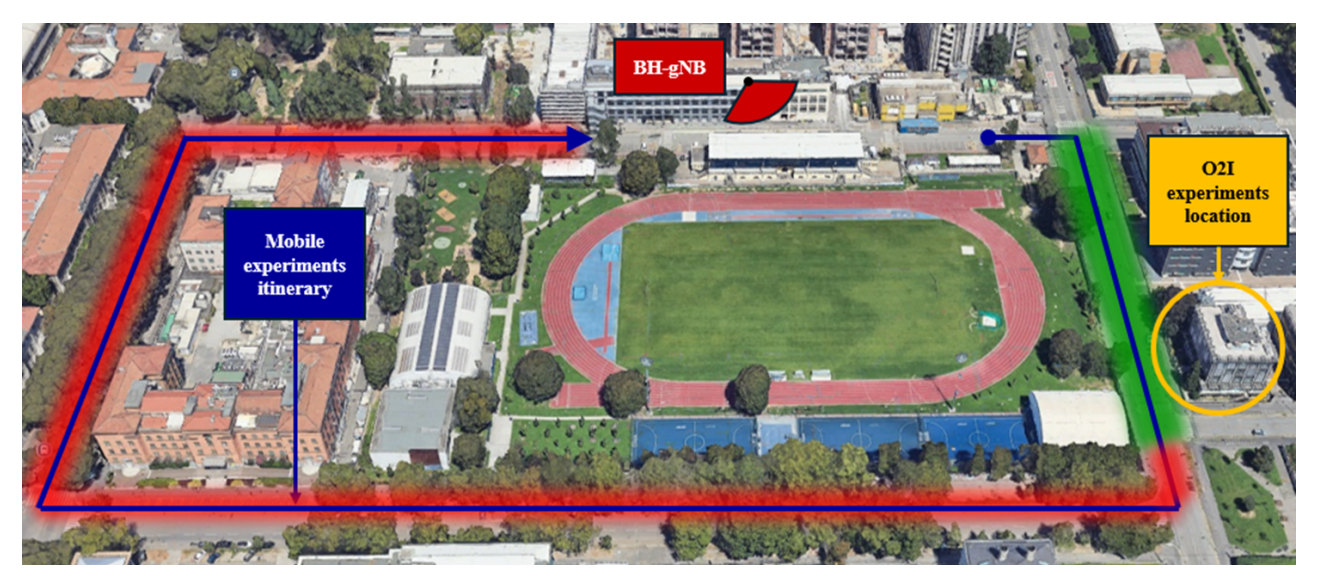


Fig. 2: Aerial view of the urban neighborhood covered by the FR2 BS together with experiment locations. Mobile experiment trajectory shows NLoS and Line of Sight (LoS) regions highlighted, respectively, in red and green.

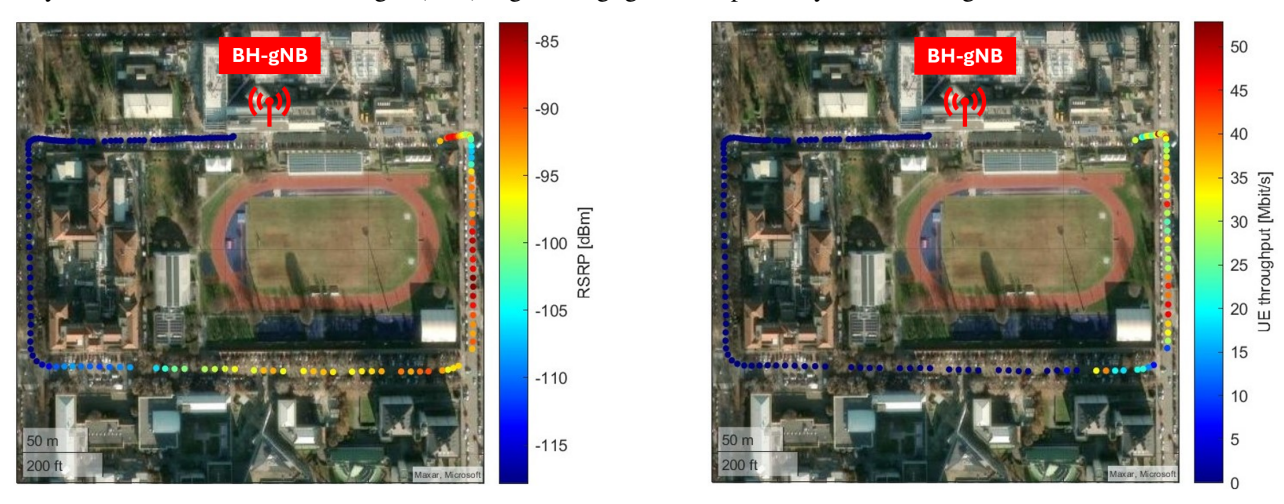


Fig. 3: Mobile WAB measurements of mmWave RSRP (on the left) and end-to-end throughput (on the right).

shows an aerial view of the urban neighborhood where the tests were performed, indicating the placement and orientation of the BH-gNB. In both scenarios, the BH-5GC and 5GC-Serving-UE were located inside the building hosting the BH-gNB, while the WAB node and end UE were moved around the area. The CPE (WAB-MT) was powered by a power bank and connected to a laptop running probe software to collect FR2 link measurements, and via Ethernet to a general-purpose machine running the OAI gNB for FR1 log acquisition through OAI logging functions. A Secure Shell (SSH) tunnel between this machine and the 5GC-Serving-UE server enabled remote execution of *iperf3* commands on both the server and the UE.

A. Mobile experiments

In this scenario, the WAB node was installed on a vehicle, with the WAB-gNB and UE placed inside and the WAB-MT (FR2 CPE) mounted on the vehicle rooftop. The vehicle moved at up to 30 km/h. Given the high directivity of the CPE antenna array and possible signal losses or reflections from the

vehicle body, the WAB-MT was mounted at the rear, with its antenna array oriented perpendicular to the ground. This setup ensured optimal reception when traveling south in the LoS area. A GPS device tracked the route and georeferenced the measurements. The chosen itinerary looped around an outdoor sports center and included segments with trees and buildings causing partial signal obstruction. End-to-end throughput measurements were performed in both Downlink (DL) and Uplink (UL) directions.

We first present the DL results. The data show that the end-to-end throughput (i.e., UE throughput) strongly correlates with the FR2 backhaul link quality. As illustrated in Fig. 3, the FR2 backhaul Reference Signal Received Power (RSRP) peaks at -83 dBm in the LoS zone, where the WAB-MT has direct visibility of the BH-gNB. In this region (until 14:45:40, as shown in Fig. 4), the end-to-end throughput reaches approximately 50 Mbps. As the vehicle moves into the NLoS area, performance gradually degrades: throughput

begins to decline when a single building obstructs the signal and eventually drops to zero in deep NLoS. This throughput degradation occurs faster than the corresponding decrease in FR2 backhaul RSRP.

This discrepancy is clarified in Fig. 4: as the end-to-end throughput decreases, the FR2 backhaul link exhibits an increasing Block Error Rate (BLER), explaining the abrupt drop in performance. The figure also reports the serving beams for both Synchronization Signal Block (SSB) and Channel State Information - Reference Signal (CSI-RS). Under LoS conditions, the wider SSB beams remain stable, whereas in NLoS regions, beam switching begins. In contrast, the narrower and more channel-sensitive CSI-RS beams continuously adjust to maintain link quality. Beam switching, however, shows no observable impact on end-to-end throughput.

During the tests, the FR1 access link operated entirely inside the vehicle, where external factors had minimal influence. The Modulation and Coding Scheme (MCS) remained stable around 27 for most of the experiment. In contrast, the FR2 segment faced more challenging conditions, with average MCS values around 20, reflecting the effects of mobility, obstructions, and environmental dynamics on the BH link.

UL measurements exhibited a trend similar to the DL results. End-to-end throughput peaked in the LoS region, matching the maximum FR2 backhaul RSRP values, and dropped rapidly as the vehicle entered NLoS. On average, the UL throughput stabilized around 1 Mbps. The notable imbalance between end-to-end DL and UL throughput primarily arises from the configuration of the mmWave backhaul segment. This setup is unfavorable for the UL direction: the 4:1 TDD frame prioritizes DL traffic, the CPE transmits at lower power than the AAU, and the maximum supported Quadrature Amplitude Modulation (QAM) order is higher in DL. Additional imbalance stems from the FR1 access segment, whose TDD scheme mirrors that of the FR2 link.

In conclusion, results from the vehicular experiments demonstrate that reliable FR2 coverage through the WAB architecture can be achieved in LoS scenarios and in NLoS regions where shadowing is not excessively severe. Moreover, the proposed approach enables widely available COTS FR1 smartphones to access an FR2 RAN without requiring costly FR2 modules.

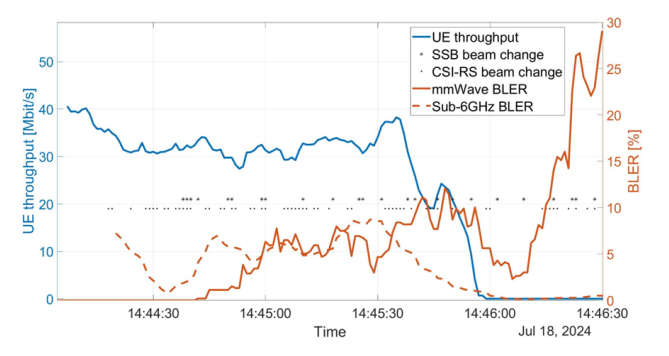


Fig. 4: End-to-end throughput, FR2 and FR1 BLER and beam changes in mobile WAB experiments.

B. O2I experiments

In this scenario, the WAB node was placed inside a building with direct visibility of the BH-gNB. End-to-end throughput measurements were conducted at five indoor positions, as shown in Fig. 5. Position 1 corresponds to a LoS condition with the BH-gNB, with only a glass facade attenuating the signal. Positions 2 and 4 are located deeper inside the building but remain subject to glass attenuation only. Positions 3 and 5, situated behind interior walls, experience additional attenuation of the incoming signal.

We first conducted FR2-only speed tests by moving the CPE through each of the five positions to assess the performance of the backhaul link. Subsequently, we assembled the WAB node and placed it at Position 1 to ensure the best possible signal conditions. We then conducted speed tests by moving the final UE, connected to the WAB node via the FR1 link, through each of the five positions. Tests were performed in both the UL and DL directions.

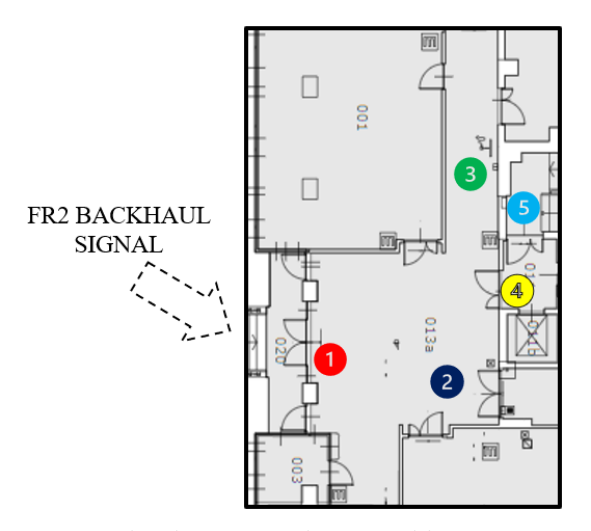


Fig. 5: O2I experiment positions.

Similarly to the mobile experiments, the directivity of the WAB-MT must be considered. During the FR2 measurements, both with and without the WAB node, the CPE was oriented in the optimal direction, as recommended in [9], to ensure maximum throughput even under NLoS conditions. This reflects the reasonable assumption that any deployed antenna array would be installed with optimal alignment.

To enable a fair comparison between the 200 MHz FR2 CPE-only scenario and the 40 MHz FR1 WAB-gNB configuration, we computed the corresponding spectral efficiency results. It is important to note, however, the substantial differences between the two implementations. The FR2 RAN is a commercial, optimized system running on dedicated hardware, operating over a 200 MHz bandwidth with a 2×2 MIMO configuration (limited by the CPE), a maximum transmit power of 37.5 dBm, and an antenna gain of 32.5 dBi. In contrast, the FR1 link is a prototype implementation based on virtualized functions running on a general-purpose machine with SDRs, operating in SISO mode with a transmit power of only 20 dBm and a basic dipole antenna. Consequently,

a significantly higher spectral efficiency is expected from the FR2 link compared to the FR1 one.

The obtained results are shown in Fig. 6a. In the DL case, as expected, the FR2-only CPE achieves significantly higher spectral efficiency than the WAB system, particularly at Positions 1 and 2, where the signal is attenuated only by glass. In the UL case, FR2 performance degrades sharply when transitioning from LoS to NLoS conditions. The WAB system also exhibits a performance drop between Position 1 and Positions 2 and 4, but the reduction is less pronounced. Notably, at Positions 3 and 5, where additional wall attenuation is present, the WAB system achieves comparable or even higher UL spectral efficiency than the FR2-only CPE. These results highlight the potential of the WAB architecture to mitigate FR2 limitations in challenging indoor NLoS environments, particularly in the uplink. Therefore, we further investigated Position 5, where the WAB system outperformed the FR2 CPE in terms of UL spectral efficiency.

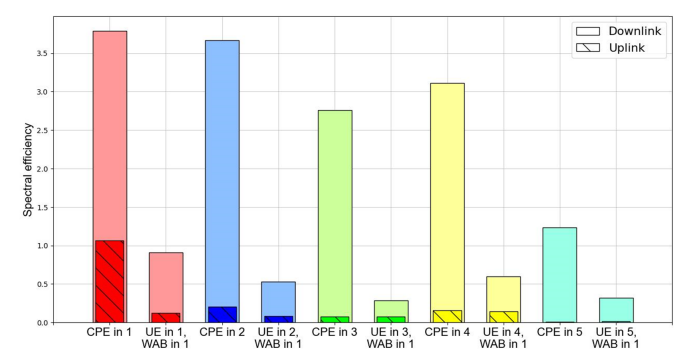
In this additional campaign, the UE was fixed at Position 5, while the WAB node was moved to Positions 2 and 4. This configuration maintained a stable backhaul link while reducing the distance between the WAB node and the UE. This adjustment had a significant impact on the FR1 access link quality, given the limitations of our testbed due to the use of prototype SDRs, the WAB-gNB operating with a low maximum transmit power, and its signal attenuating noticeably with increasing distance.

The results, reported in Fig. 6b, show a clear improvement in both DL and UL spectral efficiency as the WAB node is moved closer to the UE, highlighting the influence of access link quality. Despite the limited transmit power of the WAB-gNB, the end-to-end UL spectral efficiency of the WAB system surpasses that achieved by the FR2-only CPE. These findings confirm that the WAB architecture can effectively mitigate the typical limitations affecting FR2 UL transmissions [9], delivering enhanced performance even in challenging NLoS indoor scenarios.

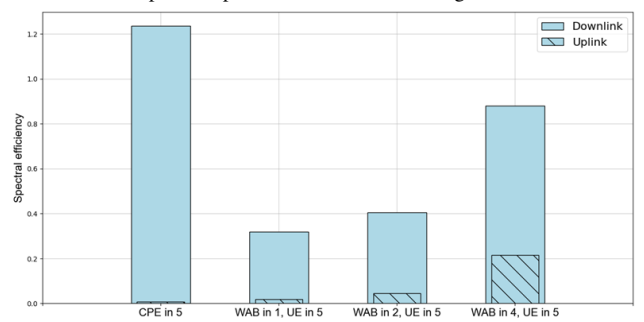
In the DL direction, the end-to-end spectral efficiency of the WAB setup remains lower than that of the FR2-only CPE. This limitation is primarily due to the prototype nature of the WAB-gNB used in our testbed. However, we expect that replacing the current FR1 configuration with a more powerful, commercial-grade FR1 system would significantly enhance downlink performance, potentially allowing the WAB architecture to outperform the FR2-only configuration even in the DL direction.

V. CONCLUSION

This paper introduced the WAB architecture as a promising enabler for wireless backhaul networks and an effective approach to exploit FR2 communications. We presented the first WAB testbed, addressing the current lack of experimental validation and providing a foundation for further research. The proposed framework, based on commercial hardware and open-source software, demonstrated through real-world measurements the advantages of relay-based systems. The WAB



(a) DL and UL SEs for each measurements positions of O2I experiments. Bar colors correspond to positions colors used in Fig. 5.



(b) DL and UL SEs of the additional indoor campaign.

Fig. 6: O2I experiments spectral efficiencies.

architecture's use of standard 5G interfaces, flexibility, and multi-band capability make it a compelling solution for next-generation networks. Future work will focus on extending the topology, improving interference and resource management, and integrating additional backhaul technologies to enhance scalability and performance.

REFERENCES

- S. Rangan et al., "Millimeter-Wave Cellular Wireless Networks: Potentials and Challenges," Proceedings of the IEEE, vol. 102, no. 3, pp. 366–385, 2014.
- [2] M. Polese et al., "Integrated Access and Backhaul in 5G mmWave Networks: Potential and Challenges," IEEE Communications Magazine, vol. 58, no. 3, pp. 62–68, 2020.
- [3] V. F. Monteiro et al., "Paving the Way Toward Mobile IAB: Problems, Solutions and Challenges," *IEEE Open Journal of the Communications Society*, vol. 3, pp. 2347–2379, 2022.
- [4] T. Tian et al., "Field Trial on Millimeter Wave Integrated Access and Backhaul," in 2019 IEEE 89th Vehicular Technology Conference (VTC2019-Spring), 2019, pp. 1–5.
- [5] R. Mundlamuri et al., "Integrated access and backhaul in 5g with aerial distributed unit using openairinterface," 2023. [Online]. Available: https://arxiv.org/abs/2305.05983
- [6] X. Lin, "The Bridge Toward 6G: 5G-Advanced Evolution in 3GPP Release 19," 2023. [Online]. Available: https://arxiv.org/abs/2312.15174
- [7] 3GPP, "Study on additional topological enhancements for NR," 3GPP, TR 38.799, version 19.0.0, 09 2024.
- [8] 3GPP, "Study on architecture enhancements for vehicle-mounted relays - Phase 2",," 3GPP, TR 23.700-06, version 19.0.0, 2024.
- [9] M. Morini et al., "Exploring Upper-6GHz and mmWave in Urban 5G Networks: A Direct on-Field Comparison," *IEEE Transactions on Mobile Computing*, pp. 1–14, 2025.
- [10] F. Kaltenberger et al., "Openairinterface: Democratizing innovation in the 5g era," Computer Networks, vol. 176, p. 107284, 05 2020.
- [11] [Online] Available: https://gist.github.com/nitred/f16850ca48c48c79bf422e90ee5b9d95.